

Petrology and Geochemistry of Granitoids of the Northern Part of Adamawa Massif, N.E Nigeria

Haruna IV*

Department of Geology, Modibbo Adama University of Technology, Yola, Nigeria

Abstract

The granitoids of the northern part of Adamawa Massif in northeastern Nigeria have been differentiated based on field and petrochemical data into the granodiorite and granites. Although there are slight mineralogical and geochemical differences between the granodiorite and the granites (e.g. Rb/Sr ratios lower in granodiorite than the granites), the two rock units have similar geochemical characteristics. The rocks are characterized by a wide range in SiO₂, Calc-alkaline affinity, syn- to within-plate granite signatures, metaluminous to peraluminous composition and more K₂O-rich and hypersthene-poor comparable to fractionated I-type granitoids. The rocks display slightly fractionated LREE, almost flat HREE patterns, with significant negative EU and Ba anomalies, Linear major element trends and progressive rise in SiO₂, K₂O, Rb and Rb/Sr ratios with depleting MgO, Fe₂O₃, CaO, TiO₂, Sr and Ba consistent with removal of plagioclase during fractionation of basic melts to yield silicic magma. This linear trend is reflected in the normative mineralogy where orthoclase and quartz increase from granodiorite to the granites whereas other minerals behave in a reverse manner.

Based on field and petrochemical features, the granodiorites and the granites of south Adamawa Massif are I-type, generated in a syn- to within-plate collision-related tectonic setting and genetically related to a common source by fractional crystallization dominated by the removal from the melt hornblende, plagioclase, biotite, K-feldspar and accessory phases such as apatite, epidote and zircon.

Keywords: Granitoids; Adamawa massif; Petrology; Geochemistry

Introduction

Adamawa Massif consists largely of granitoids and migmatites-gneisses complex (Figure 1) [1]. It is situated in eastern Nigeria and lies in an extensive area between the Benue Trough to the west and the Cameroon Line to the east. To the north, it is bordered by Hawal Massif and to the south, by Oban Massif (Figure 2) [2]. The three massifs extend into the Republic of Cameroon and form the Eastern Nigerian Basement Complex which is one of the three major basement complexes in Nigeria. The Oban Massif has been extensively studied [3-8]. Similarly the Hawal has recently received the attention of Bassey, Obiefuna et al and Baba [9-11]. Unlike its Oban and Hawal equivalents, little is known about the geology of Adamawa Massif and there is hardly any data on the major, trace and rare earth elements contents of these rocks. The scarcity of such data probably led Ogunleye and Okujeni [12] to believe that the pockets of uranium in the sub adjacent Benue Trough were sourced from the volcanics within the Trough even though no evidence of uranium enrichment in these volcanics has been documented. Again, because of the paucity of research work on this massif, there is always a tendency to infer the geology of Adamawa Massif from that of the well-studied Oban Massif. This has always led to erroneous conclusions.

This paper combines field with major, trace and rare earth elements petrochemical data to expand information on the origin and tectonic environment of the basement geology of Adamawa Massif.

Regional Geological Setting and Tectonics

Nigeria is situated within the Pan African mobile belt and sandwiched between the West African Craton to the west, the Taureq shield to the north and the Congo Craton to the southeast (Figure 2) [2]. Opinions are divided concerning the evolution of the Nigerian Pan African terrain. The first and most popular opinion is that the Nigerian Pan African terrain is the result of tectonic processes involving continental collision between West African Craton and the Pan African mobile belt [13-17]. The resultant heat, deformation and partial melting of the upper mantle and lower crust led to the emplacement of the

granites. This interpretation is based on the recognition of a suture along the eastern margin of the West African Craton. The second opinion suggests that the Pan African orogeny was more of aggregation of crustal blocks such as island arcs and older continental fragments than a simple collision between two entities – the West African Craton and the Pan African mobile belt [18-21]. This interpretation is predicated on the close association of calc-alkaline volcanics, ultramafic and basic rocks with the two major NE-SW trending fracture systems established in the western part of Nigeria.

Even though the former opinion has been widely accepted, some workers have observed that the Pan-African granites which extend to Nigeria and Cameroon, a distance of over 1500 km from the suture cannot be related to the same subduction zone [22,23].

The Granitoids

The granitoids of the study area are classified as granites and granodiorite based on the chemical classification of Cox et al. [24]. Such classification is consistent with the QAPF classification based on modal proportions of constituent minerals [25]. The granites are further subdivided based on field characteristics into migmatites, equigranular granite, porphyritic granite and fine-grained granite.

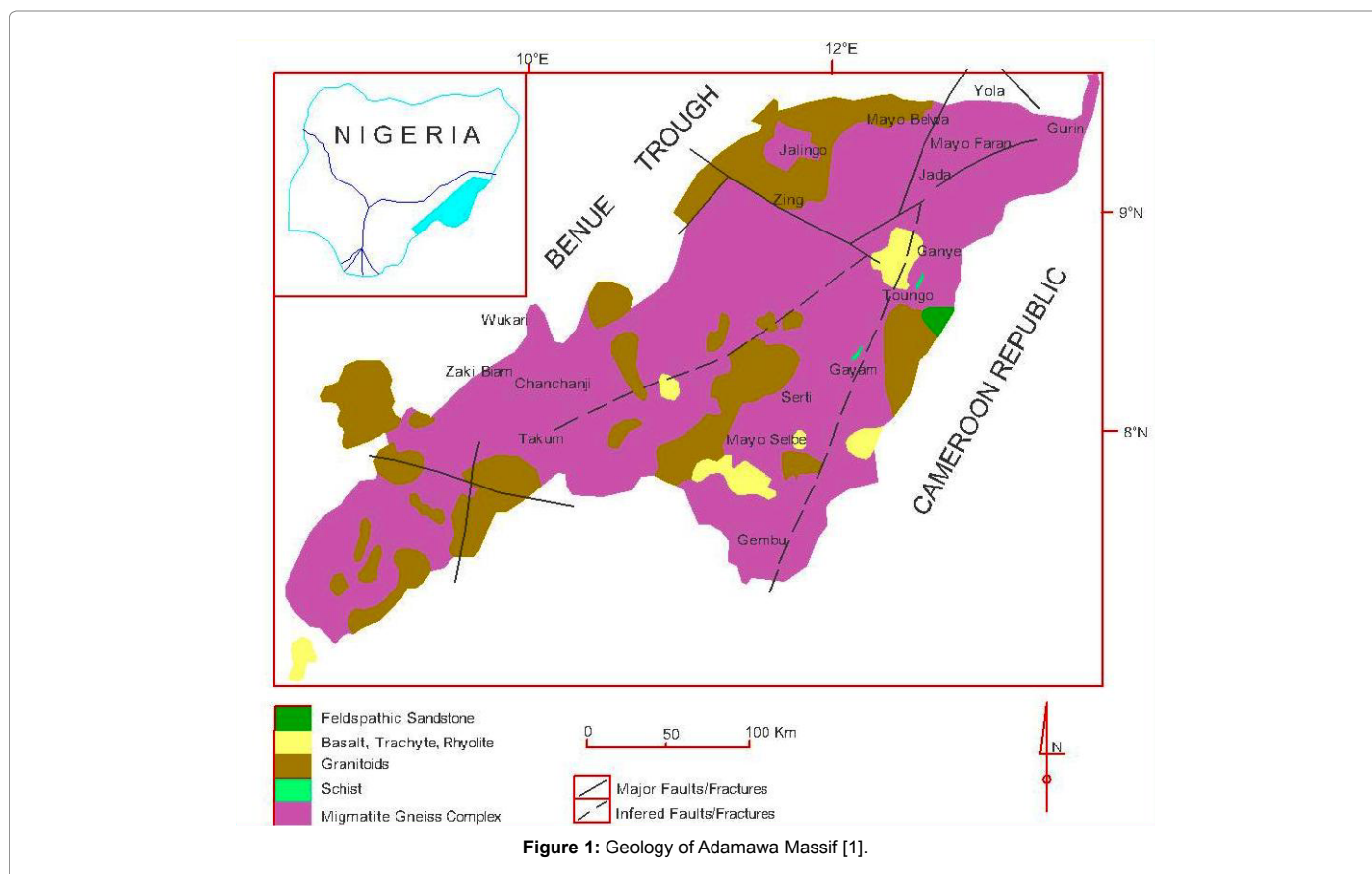
The granodiorite presents a wide range in composition from basic granodiorite to quartz monzonite or adamellite. Distinction (in the field) between the various members of the group is difficult as they

*Corresponding author: Haruna IV, Department of Geology, Modibbo Adama University of Technology, Yola -Nigeria, Tel: 08124816318; E-mail: vela_hi@yahoo.co.uk

Received August 08, 2014; Accepted October 24, 2014; Published November 03, 2014

Citation: Haruna IV (2014) Petrology and Geochemistry of Granitoids of the Northern Part of Adamawa Massif, N.E Nigeria. J Geol Geosci 3: 177. doi: 10.4172/2329-6755.1000177

Copyright: © 2014 Haruna IV. This is an open-access article distributed under the terms of the Creative Commons Attribution License, which permits unrestricted use, distribution, and reproduction in any medium, provided the original author and source are credited.



frequently grade into one another. They were therefore mapped as granodiorite. Granodiorite is distinguished from other rock units in the field by its fairly high mafic mineral content and its pronounced grayish colour. This greyish appearance strongly contrasts with the pink and pale red of the granites.

The granites are similar in mineral composition but vary texturally and structurally and include the migmatites, equigranular granites, porphyritic granites and fine-grained granites. Migmatites are of restricted occurrence in the area. They consist of granitic materials alternating with biotite-enriched mafic materials. They are poorly foliated, mostly leucocratic, coarse-grained and show considerable variations in structure, texture and and to a lesser extent, mineralogy. All phases of transition are observed between the variants which probably reflect the composition and physical conditions of the original country rock and various degrees of granitisation. Biotite and iron ore minerals are the sole ferromagnesian minerals. Pegmatitic segregations, patches of granites and xenoliths of mafic rocks are very conspicuous in the migmatites. The granitic portion of the migmatite is often leucocratic and medium- to coarse-grained.

Equigranular granites are next in abundance only to porphyritic granites which are the most abundant rock type in the area. They are medium-grained (mineral grains of the order 3 mm×3 mm) and include a diverse series of granites varying slightly in texture, structure and mineralogy. Contacts between the various types are mostly gradational. The equigranular granites are massive in some places and foliated in others. The foliation is expressed by elongate biotite and to lesser extent feldspar and quartz crystals.

Essential minerals occurring in equigranular granites include

feldspar, quartz and biotite. Sericite and iron ore minerals constitute the alteration products.

The most striking characteristic of porphyritic granites is their porphyritic texture consisting of phenocrysts of microcline (mineral grains in the size range 20 mm×30 mm to 35 mm×40 mm) set in a medium- to coarse-grained mineral matrix ranging in size from 2 mm×3 mm to 4 mm×5 mm. They are relatively homogeneous, having predominantly gradational contacts (transitional) and restricted sharp contacts with equigranular granites and migmatite. These rocks are mainly potash granites, which grade into a fairly basic variety at the margins of the intrusions. Composition and texture of porphyritic granite changes as one traverse the intrusions from the center to the borders (margins). At the center, feldspar phenocrysts are crowded and the rock appears to be homogeneous biotite granite. This composition gradually changes to what appear to be syenite and monzonites at the margins, where the density of feldspar phenocryst is less.

The fine-grained granites are pale brown to grey, dominantly equigranular, fine-grained and show little variation in appearance. The rock consists of predominantly quartz, microcline and plagioclase. Similar rock forms enclaves which occur as irregular bodies and as vein-like lenses within the equigranular granites. In some places, veins of fine-grained granite interfinger and penetrate the porphyritic granites. Fine-grained granite, like the migmatite, is of subordinate occurrence in the study area.

Sampling and Analytical Procedure

The sampling procedure involved the collection of at least three individual samples of fresh rock from each outcrop. The samples, each

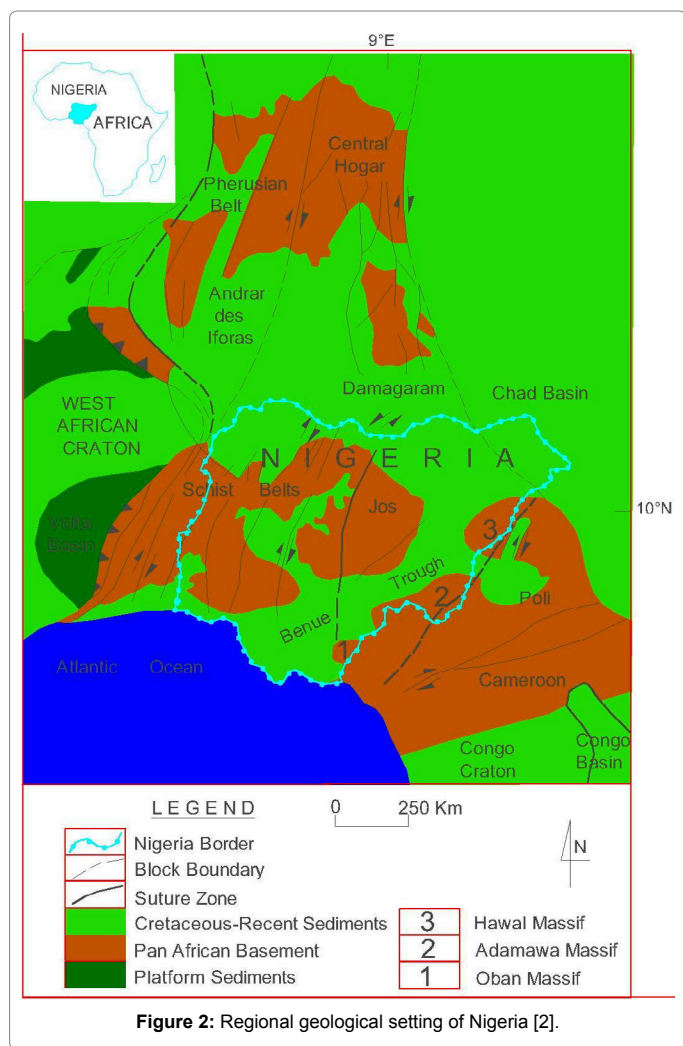


Figure 2: Regional geological setting of Nigeria [2].

weighing about 5 kg, were subjected to preliminary preparation at the geochemical laboratory of Ashaka Cement Company. Each sample set was first crushed and manually sorted to obtain representative sample. Each representative sample was then pulverised in a disc mill. Finally the powdered samples were packaged, labelled and shipped to Activation Laboratory (ACTLABS), Canada where the samples were analysed for major elements using ICP and the trace elements and Rare Earth Elements using fusion ICP/MS package. The samples locations are shown in Figure 3 while the major and trace elements data contents for the granitoids are given in Table 1 and the normative mineralogy calculated therefrom presented on Table 2. Part of this data was earlier used by the authors to constraint the origin and processes of uranium in the northern part of Adamawa Massif.

Geochemistry

Major elements distinctions between the granites are subtle, however, the average granite has higher SiO₂, K₂O, Na₂O, Rb and lower MgO, CaO, TiO₂, Fe₂O₃(t), Al₂O₃, Ba and Sr than the granodiorites. Collectively, the granitoids have a wide range of SiO₂ (64.75 to 76.27 wt%), MgO (0.01 to 1.40 wt%), CaO (0.58 to 3.66 wt%), TiO₂ (0.02 to 1.44 wt%), Fe₂O₃, (0.46 to 8.20 wt%), MnO, (0.01 to 0.12 wt%), and a relatively narrow range of Al₂O₃ (12.91 to 16.37 wt%), Na₂O (2.46 to 4.28 wt%), K₂O (4.24 to 6.36 wt%).

In general, major and trace elements displayed display continuous trends with MgO, CaO, and Fe₂O₃ abundances decreasing with increasing SiO₂. Similarly, Sr and Ba decrease steadily with increasing SiO₂ while on the contrast, K₂O and Rb increase with increasing SiO₂. The remaining elements exhibit no clear patterns (Figure 4). There is clear absence of separate groups among the granites.

In general, the granitoids are characterized by very little foliation, mafic enclaves in granodiorite, low normative corundum (<1% in most samples), calc-alkaline affinity (Figure 5) [26], high Na₂O contents (generally more >3.5%), Al/Na₂O+CaO contents of ≤ 1.1 wt%, moderate values of Rb, Ba, LREE and Rb/Sr ratios. All these features, according to the nomenclature of Chappell and White [27] are typical of I-type granites.

On the SiO₂ versus Nb diagram of Kleeman and Twist [28] the granitoids plot in the orogenic field (Figure 6) [28]. A plot of A/NK versus Al saturation index (ASI) [Al₂O₃/(Na₂O+K₂O+CaO)] shows that the granitoids are metaluminous to peraluminous (Figure 7) [29]. On TiO₂ (wt %) versus Al₂O₃/TiO₂ diagram (Figure 8) [30] the plot indicates one curvilinear trend for all the granitoids characteristic of magmatic differentiation.

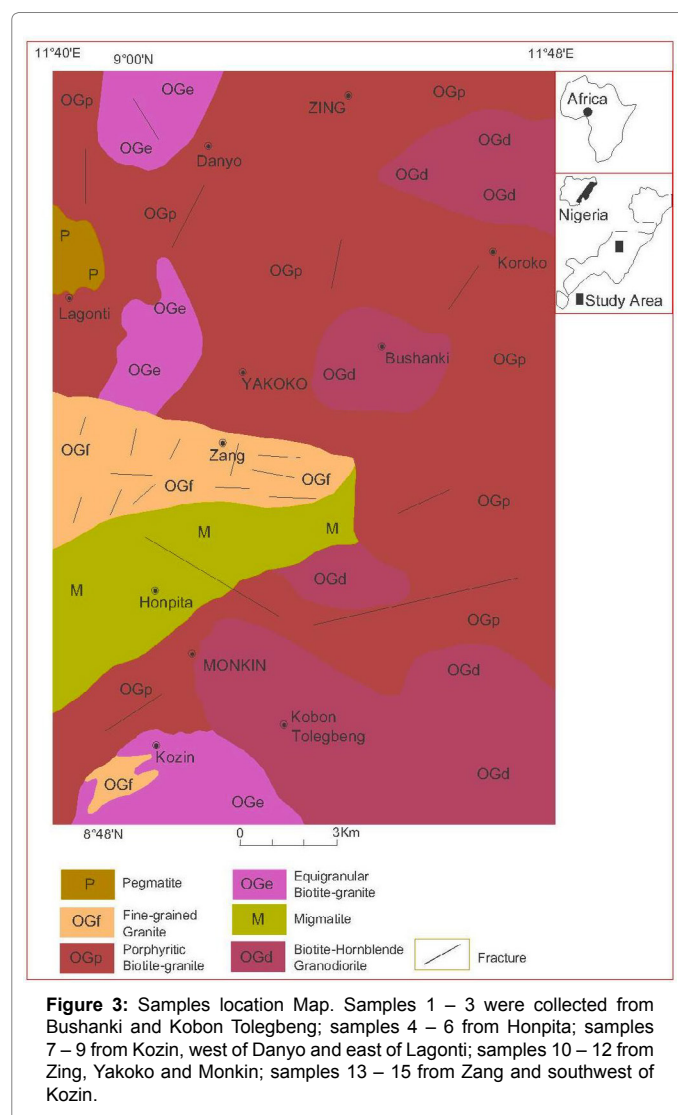


Figure 3: Samples location Map. Samples 1 – 3 were collected from Bushanki and Kobon Tolegbeng; samples 4 – 6 from Honpita; samples 7 – 9 from Kozin, west of Danyo and east of Lagonti; samples 10 – 12 from Zing, Yakoko and Monkin; samples 13 – 15 from Zang and southwest of Kozin.

Major Elements	1	2	3	4	5	6	7	8	9	10	11	12	13	14	15
SiO ₂	65.97	65.68	64.75	72.25	69.86	67.88	73.48	76.27	73.71	72.53	76.27	72.26	75	74.61	74.32
Al ₂ O ₃	16.37	16.15	13.52	13.62	14.48	15.75	13.2	13.51	13.25	12.91	13.3	14.81	13.6	13.85	13.65
Fe ₂ O ₃ (T)	3.46	4	8.2	3.18	2.86	2.46	2.17	0.46	1.88	3.15	0.59	1.38	1.52	1.57	1.52
MnO	0.073	0.08	0.121	0.042	0.044	0.028	0.031	0.005	0.04	0.043	0.019	0.024	0.031	0.027	0.034
MgO	1.34	1.4	1.15	0.29	0.57	0.71	0.13	0.01	0.18	0.24	0.02	0.3	0.19	0.19	0.2
CaO	2.33	2.48	3.66	1.58	1.54	2.23	0.81	0.58	1.13	1.45	0.83	1.46	1.01	1.09	1.05
Na ₂ O	4.18	4.28	2.71	2.65	3.52	3.75	3.11	3.9	2.89	2.46	4.12	3.49	3	3.09	3.02
K ₂ O	4.76	4.24	4.32	6.37	5.49	5.16	6.06	5.28	5.66	6.01	4.51	5.92	5.6	5.81	5.57
TiO ₂	0.704	0.727	1.444	0.46	0.389	0.548	0.198	0.019	0.18	0.381	0.039	0.226	0.164	0.161	0.165
P ₂ O ₅	0.28	0.3	0.48	0.11	0.11	0.15	0.05	0.01	0.05	0.09	0.02	0.08	0.04	0.05	0.05
LOI	0.52	0.56	0.24	0.43	0.4	0.42	0.5	0.33	0.48	0.36	0.17	0.52	0.47	0.44	0.45
Total	99.97	99.88	100.6	101	99.27	99.09	99.74	100.4	99.47	99.64	99.9	100.5	100.6	100.9	100
Trace Elements															
Sc	11	12	16	7	4	3	3	2	4	6	3	1	3	3	3
Be	12	11	3	2	3	2	3	6	4	2	4	3	3	3	3
V	61	70	68	14	22	40	<5	<5	5	10	<5	21	5	9	6
Ba	1590	1254	1073	1012	786	1832	393	22	444	1078	36	1333	465	464	472
Sr	495	479	251	164	233	685	96	11	106	172	17	440	126	131	130
Y	33	33	63	62	27	11	24	45	98	47	22	13	14	18	32
Zr	213	268	569	480	266	297	293	67	196	393	49	136	129	140	123
Cr	<20	<20	<20	<20	<20	<20	<20	<20	<20	<20	<20	<20	<20	<20	<20
Co	17	14	23	13	15	15	14	18	17	16	18	19	11	14	15
Ni	<20	<20	<20	<20	<20	<20	<20	<20	<20	<20	<20	<20	<20	<20	<20
Cu	<10	<10	<10	<10	10	<10	<10	<10	<10	<10	<10	<10	<10	10	<10
Zn	70	90	140	60	50	60	40	<30	40	80	<30	<30	<30	40	30
Ga	27	27	27	27	26	22	21	29	24	25	23	21	20	20	21
Ge	1	1	2	2	1	<1	1	2	2	2	1	1	1	1	1
As	<5	<5	<5	<5	<5	<5	<5	<5	<5	<5	<5	<5	<5	<5	<5
Rb	234	250	175	250	224	158	210	368	310	230	290	206	286	294	299
Nb	22	23	34	30	15	12	11	42	24	26	16	8	15	14	15
Mo	<2	<2	<2	<2	<2	<2	3	<2	<2	<2	<2	<2	<2	<2	<2
Ag	<0.5	<0.5	<0.5	<0.5	<0.5	<0.5	<0.5	<0.5	<0.5	<0.5	<0.5	<0.5	<0.5	<0.5	<0.5
In	<0.2	<0.2	<0.2	<0.2	<0.2	<0.2	<0.2	<0.2	<0.2	<0.2	<0.2	<0.2	<0.2	<0.2	<0.2
Sn	4	5	5	3	3	4	3	2	7	4	3	4	5	5	5
Sb	<0.5	<0.5	<0.5	<0.5	<0.5	0.9	0.6	<0.5	<0.5	0.9	<0.5	<0.5	<0.5	1.5	<0.5
Cs	8.4	10.8	1.6	0.9	2.3	1.1	2.7	2.4	2.9	1.6	3.7	2.6	6	6.3	5.9
Hf	5.2	7.5	13.5	14.1	7.2	7.3	7.5	3.9	5.8	11.4	2.2	3.6	3.9	4.3	3.9
Ta	3.9	3.9	2.7	1.8	1.5	0.8	0.7	6.2	2.3	1.9	1.3	1.2	2	1.8	1.8
W	65	46	80	77	85	82	94	121	115	109	134	124	74	96	105
Tl	1.2	1.8	1.2	1.4	1.3	1.6	1.8	1.7	1.7	1.8	2.1	1.2	2.2	3.1	2.3
Pb	15	22	17	22	18	42	25	36	26	34	42	22	32	49	32
Bi	<0.4	<0.4	<0.4	<0.4	<0.4	<0.4	<0.4	<0.4	<0.4	<0.4	<0.4	<0.4	<0.4	<0.4	<0.4
Th	12.5	14.5	28.6	61.3	37.8	25.2	35.9	15.3	56.6	45.7	27.5	30.8	28.9	37.4	47
U	2.6	2.4	2.2	2.6	3	2.4	2.4	8.6	5	2.3	5	1.6	4.6	4.9	5.3
REE															
La	49.3	51.6	103	203	86.7	66.1	82	8.1	78.5	185	4.6	38.6	40.4	48.2	57.8
Ce	114	122	228	411	140	130	168	11.9	176	368	9.7	72.9	87.3	99.5	120
Pr	13.3	13.1	25.9	44.5	17.1	13.8	17.8	2.05	19.4	38.4	1.37	6.86	9.15	10.9	12.4
Nd	44.8	48.3	89.1	143	53.3	39.5	54.7	10.9	65.2	122	7.9	20	30.1	36.8	43.8
Sm	9.4	10.6	18.4	29	10.4	6.7	9.9	3.5	13.6	21.9	2.9	3.3	6	7.2	8.7
Eu	1.95	2.12	2.82	2.21	1.32	1.42	0.85	0.13	0.84	2.31	0.16	0.76	0.56	0.59	0.6
Gd	7.7	7.6	15	18.7	7.2	3.6	6.7	5.3	12.6	13.8	3.3	2.6	3.9	4.9	6.7
Tb	1.1	1.1	2.1	2.5	1	0.4	0.9	1.2	2.2	1.8	0.6	0.4	0.6	0.7	1.1
Dy	5.6	6	11	13.2	5.1	2	4.9	8.4	13.2	9.4	4.1	2	3	3.7	6.4
Ho	1.1	1.2	2.1	2.4	1	0.4	0.9	1.9	2.9	1.8	0.8	0.4	0.5	0.7	1.4
Er	3.3	3.4	6.3	6.6	3.1	1.1	2.4	5.8	9.6	5.1	2.5	1.3	1.6	1.9	4.5
Tm	0.52	0.5	0.88	0.87	0.44	0.16	0.34	0.93	1.53	0.68	0.37	0.22	0.24	0.27	0.69
Yb	3.2	3	5.2	4.6	2.4	1.1	2.1	5.9	9.7	3.8	2.2	1.5	1.5	1.8	4.3
Lu	0.41	0.42	0.69	0.6	0.31	0.16	0.29	0.84	1.3	0.52	0.32	0.21	0.25	0.29	0.65
(Tb/Yb)N	1.46	1.56	1.72	2.31	1.77	1.55	1.82	0.87	0.97	2.02	1.16	1.13	1.70	1.65	1.09
(La/Yb)N	9.34	10.42	12.00	26.75	21.9	36.42	23.67	0.83	4.90	29.5	1.27	15.60	16.3	16.2	8.15
(La/Sm)N	2.88	2.67	3.07	3.84	4.57	5.41	4.54	1.27	3.17	4.63	0.87	6.42	3.69	3.67	3.64
Eu/Eu*	0.68	0.69	0.50	0.27	0.44	0.80	0.30	0.09	0.19	0.38	0.16	0.77	0.33	0.29	0.23

Sample 1 – 3 = granodiorite; sample 4 – 6 = migmatite; sample 7 – 9 = equigranular granite; sample 10 – 12 = porphyritic granite; sample 13 – 15 = fine-grained granite.

Table 1: Major (wt%) and Trace Elements (ppm) Analyses of the granitoids of north Adamawa Massif.

Mineralsar	1	2	3	4	5	6	7	8	9	10	11	12	13	14	15
Apatite	0.66	0.71	1.14	0.26	0.26	0.36	0.12	0.02	0.12	0.21	0.05	0.19	0.09	0.12	0.12
Pyrite	0	0	0	0	0	0	0	0	0	0	0	0	0	0	0
Chromite	0	0	0	0	0	0	0	0	0	0	0	0	0	0	0
Fluorite	0	0	0	0	0	0	0	0	0	0	0	0	0	0	0
Calcite	0	0	0	0	0	0	0	0	0	0	0	0	0	0	0
Zircon	0.04	0.05	0.11	0.1	0.05	0.06	0.06	0.01	0.04	0.08	0.01	0.03	0.03	0.03	0.02
Ilmenite	0.16	0.17	0.26	0.09	0.09	0.06	0.07	0.01	0.09	0.09	0.04	0.05	0.07	0.06	0.07
Sphene	0	0	2.36	0.65	0	0	0	0	0	0.31	0	0	0	0	0
Orthoclase	28.13	25.06	25.53	37.64	32.44	30.49	35.81	31.2	33.45	35.52	26.65	34.98	33.09	34.33	32.92
Albite	35.37	36.22	22.93	22.42	29.78	31.73	26.32	33	24.45	20.82	34.86	29.53	25.38	26.15	25.55
Aegerine	0	0	0	0	0	0	0	0	0	0	0	0	0	0	0
Anorthite	10.21	10.75	11.97	6.46	7.16	10.67	3.8	2.82	5.4	6.43	4	7.13	4.88	5.22	5.02
Corundum	0.6	0.58	0	0	0.12	0.08	0.13	0.35	0.39	0	0.18	0.05	0.81	0.57	0.81
Magnetite	0	0	0	0	0	0	0	0	0	0	0	0	0	0	0
Hematite	4.46	4	8.2	3.18	2.86	2.46	2.17	0.46	1.88	3.15	0.59	1.38	1.52	1.57	1.52
Diopside	0	0	0	0	0	0	0	0	0	0	0	0	0	0	0
Hypersthene	3.34	3.49	2.86	0.72	1.42	1.77	0.32	0.02	0.45	0.6	0.05	0.75	0.47	0.47	0.5
Wollastonite	0	0	0	0	0	0	0	0	0	0	0	0	0	0	0
Quartz	17.02	17.81	24.81	29.01	24.42	20.63	30.34	32.14	32.62	31.96	33.29	25.77	33.72	31.86	32.96
Olivine	0	0	0	0	0	0	0	0	0	0	0	0	0	0	0
Perovskite	0	0	0	0	0	0	0	0	0	0	0	0	0	0	0
Rutile	0.62	0.64	0.35	0.15	0.34	0.52	0.16	0.01	0.14	0.2	0.02	0.2	0.13	0.13	0.13
Nepheline	0	0	0	0	0	0	0	0	0	0	0	0	0	0	0
Leucite	0	0	0	0	0	0	0	0	0	0	0	0	0	0	0
Ca_Orthosilicate	0	0	0	0	0	0	0	0	0	0	0	0	0	0	0
Kaliophilite	0	0	0	0	0	0	0	0	0	0	0	0	0	0	0
Na ₂ SiO ₃	0	0	0	0	0	0	0	0	0	0	0	0	0	0	0
K_Meta	0	0	0	0	0	0	0	0	0	0	0	0	0	0	0
Acmite	0	0	0	0	0	0	0	0	0	0	0	0	0	0	0
Wt%_Oxides	100.7	99.6	100.6	100.7	99	99	99.3	100.1	99.1	99.5	99.7	100.2	100.2	100.5	99.7
Wt% Phase	100.6	99.5	100.5	100.70	99.00	98.80	99.30	100.10	99.00	99.40	99.70	100.10	100.20	100.50	99.60
D.I	80.52	79.09	73.27	89.07	86.64	82.85	92.47	96.34	90.52	88.3	94.8	90.28	92.19	92.34	91.43

Sample 1 – 3 = granodiorite; sample 4 – 6 = migmatite; sample 7 – 9 = equigranular granite; sample 10 – 12 = porphyritic granite; sample 13 – 15 = fine-grained granite.

Table 2: CIPW normative minerals (%) of the granitoids of Zing-Monkin area.

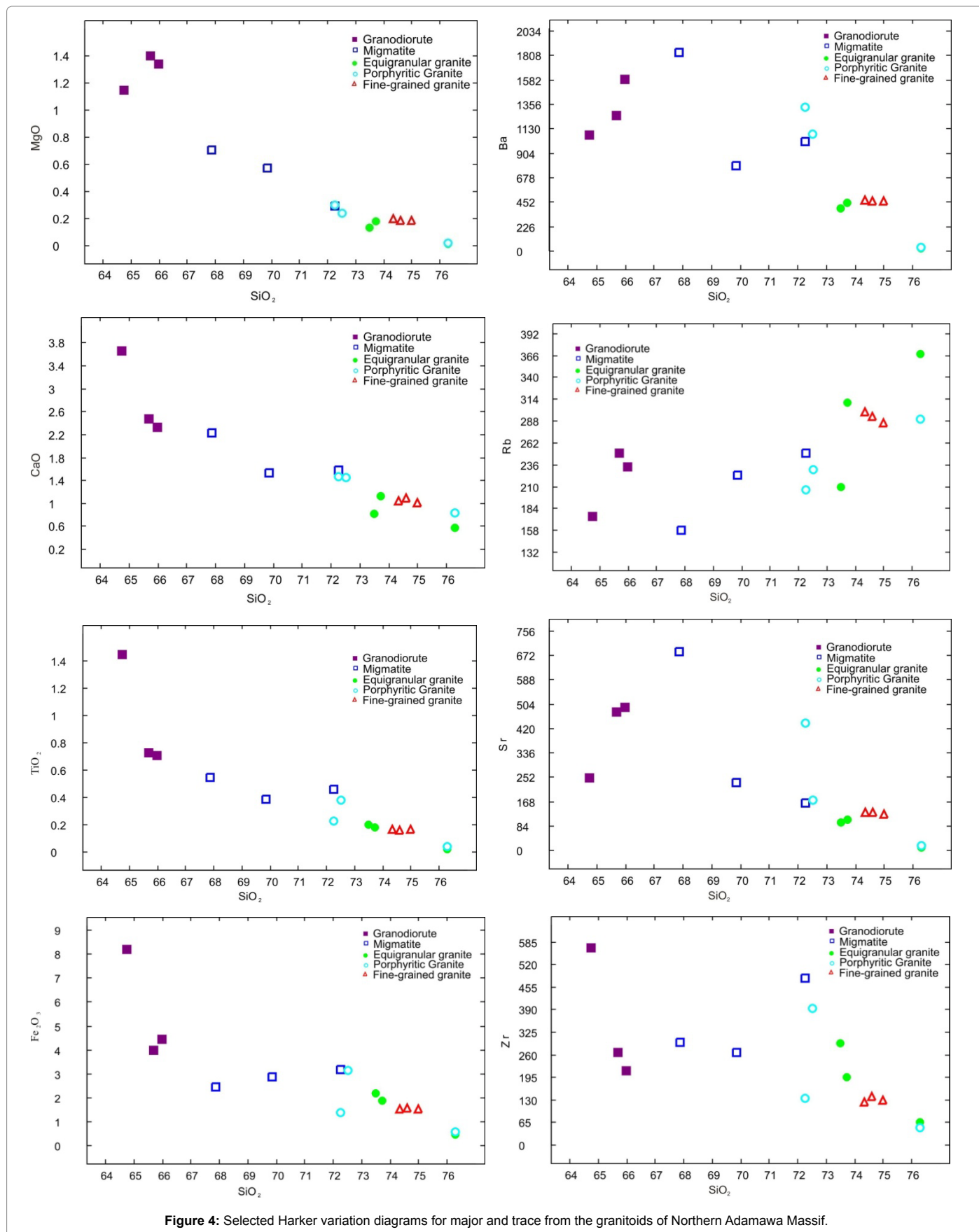
Plots of REE data for the granitoids on chondrite-normalised diagram of Boynton [31] display smooth coherent patterns from La to Lu. The REE distribution patterns for individual rock units (although not separately shown here) vary only slightly. The granodiorite displays fractionated REE patterns [(La/Yb)_N = 10.59 on average], slightly fractionated LREE enriched pattern [(La/Sm)_N = 2.87 on the average] and an almost flat HREE [(Tb/Yb)_N = 1.58 on the average] with very small negative Eu anomalies (Eu/Eu* = 0.69 on the average). REE abundances in the granites are characterised by strongly fractionated patterns [(La/Yb)_N = 16.80 on average] with a strongly fractionated LREE-enriched patterns [(La/Sm)_N = 4.81 on the average]. They display a near flat HREE pattern [(Tb/Yb)_N = 1.48 on average] and exhibits appreciable negative Eu anomalies (Eu/Eu* = 0.44 on average). A combined chondrite-normalised diagram (Figure 9) [32] for the granitoids of the study area shows that the REE abundances are characterised by fractionated patterns [(La/Yb)_N = 15.55 on average] and displays strongly fractionated LREE-enriched trends [(La/Sm)_N = 3.62 on average] with less fractionated HREE patterns [(Tb/Yb)_N = 1.52 on average] and significant negative Eu anomalies (Eu/Eu* = 0.41 on average). Trace elements distributions in which concentrations are normalised to average continental crust according to Weaver and Tarney [33] (Figure 10), may reflect the primary features of the melts and therefore give a general indication of the tectonic setting. On Figure 9 therefore, the granitoids are characterized by enrichment in Rb, Th and Nb and have high Y and Yb with pronounced negative EU anomalies.

Collectively, this trend resembles that of post-collisional granites [34-36].

Discussion

Origin of the granitoids of zing-monkin area

Mantle and crust are two end member sources of granitoids. However, the two sources are not mutually exclusive. While most granitic rocks originate by contribution from both sources, some are derived purely from the end member sources [36,37]. The composition of the source and the physico-chemical processes that affect this source and the melt therefore control the chemistry of granitic rocks. Such characteristics have been described by Chappell and White [38]. Petrological and petrochemical investigation of the granitoids of the study area has led to recognition of two distinct granitoids types: the granodiorite and the granites (texturally subdivided into migmatite, equigranular granite, porphyritic granites and the fine-grained granites). The relatively uniform composition and overlapping ranges in most of their major, trace and rare earth elements contents indicates that they might have been derived from similar parental magma source. This notion of a genetic relationship is demonstrated on a plot of TiO₂ versus Al₂O₃/TiO₂ (Figure 7). The curvilinear trend for all the rock units is typical of magmatic differentiation and suggests that the rocks were generated from a chemically similar magma source [30]. It also suggests that the variation in the granitoids is probably the result



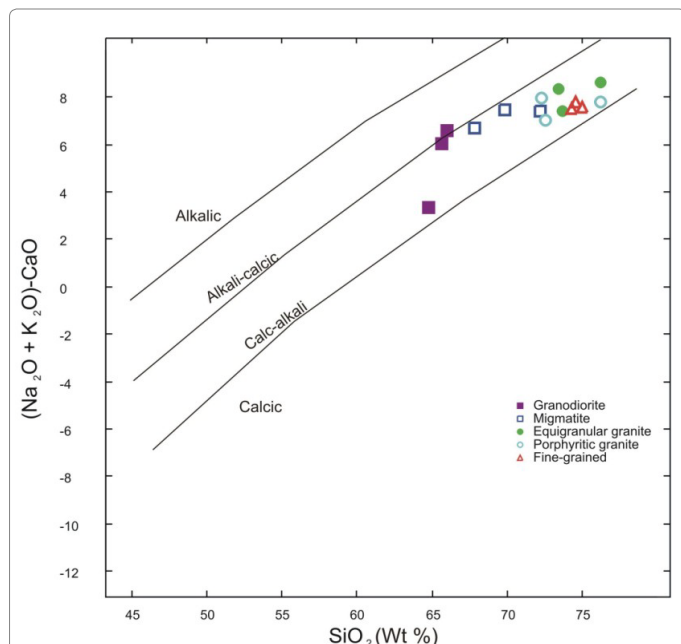


Figure 5: Subdivision of the granitoids of Northern Adamawa Massif according to the modified alkali-lime index of Frost BR, Barnes CG, Collins WJ [26] as given by a plot of $(\text{Na}_2\text{O} + \text{K}_2\text{O}) - \text{CaO}$ versus SiO_2 .

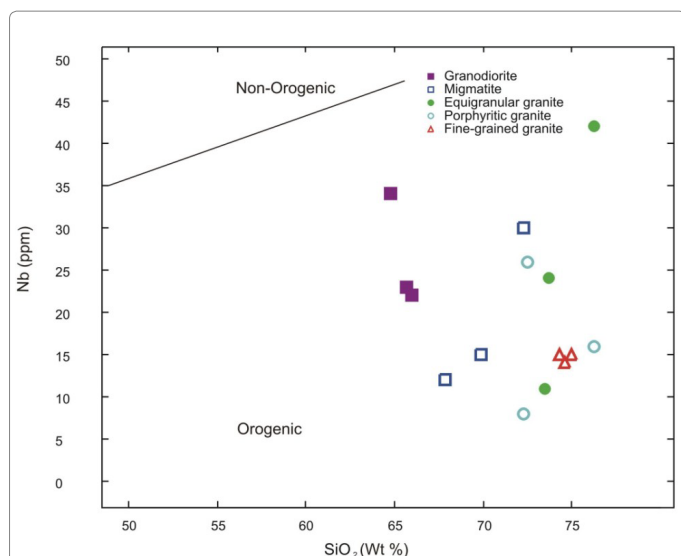


Figure 6: SiO_2 (wt %) versus Nb(ppm) variation plot for the granitoids Northern Adamawa Massif [28].

of hybridization between the original magma and amphibolitic cover rocks [39]. Major and Rare earth elements chemistry of the granitoids suggest an evolutionary sequence from the more mafic granodiorite to the more evolved granites. Granitoids may be formed by fractional crystallization of mantle derived magmas, anatexis of crustal rocks or a combination of the two processes. Generally, there is an appreciable Eu anomalies ($\text{Eu}/\text{Eu}^* = 0.41$ on the average) probably produced by the removal of plagioclase consistent with fractionation of basic melts to yield silicic magmas. Liquids generated from melting of greywackes are of trondhjemitic composition and have low Al_2O_3 , K_2O , Ba and Rb contents [40]. Enrichment of these major and trace elements in the

investigated granitoids argues against its formation by the melting of possible greywackes.

Geochemical modeling of Rb/Sr during melting suggest that a fluid present melting reaction of muscovite + plagioclase + quartz would

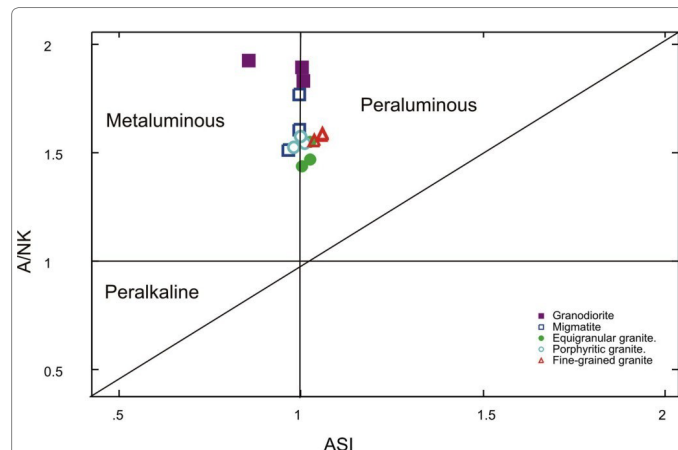


Figure 7: A/NK Vs ASI of Zen for the granitoids of Northern Adamawa Massif [29].

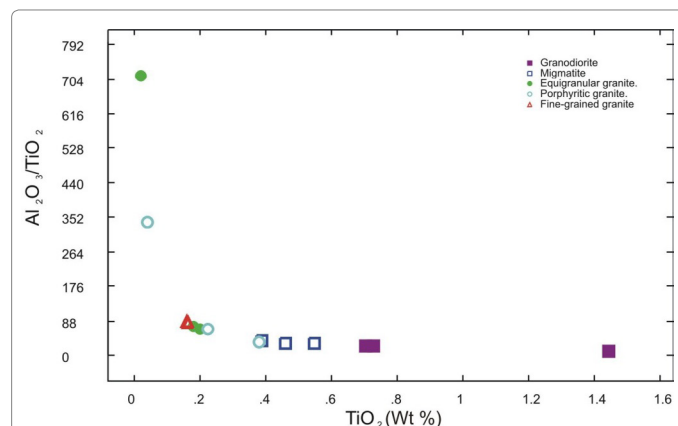


Figure 8: TiO_2 (wt %) versus $\text{Al}_2\text{O}_3/\text{TiO}_2$ variation plots for the granitoids Northern Adamawa Massif [30].

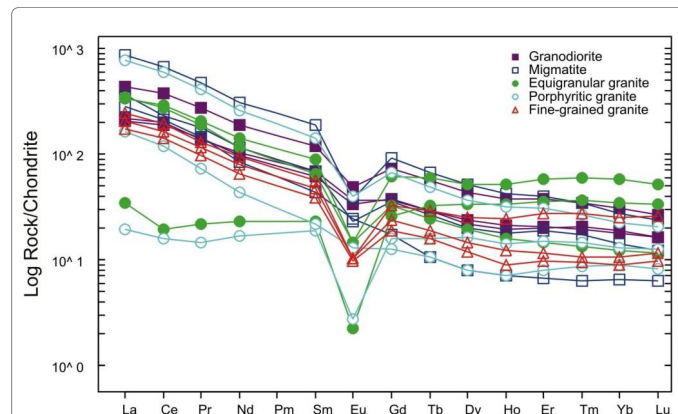


Figure 9: Chondrite-normalised REE abundances for the granitoids Northern Adamawa Massif using the normalizing values of Sun and McDonough [32].

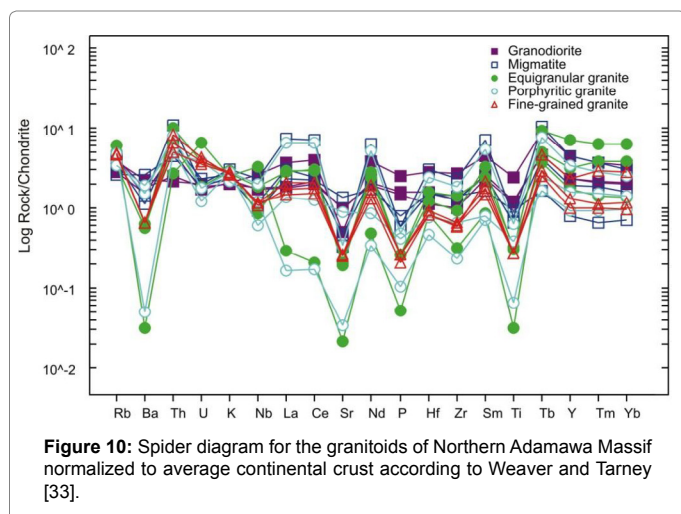


Figure 10: Spider diagram for the granitoids of Northern Adamawa Massif normalized to average continental crust according to Weaver and Tarney [33].

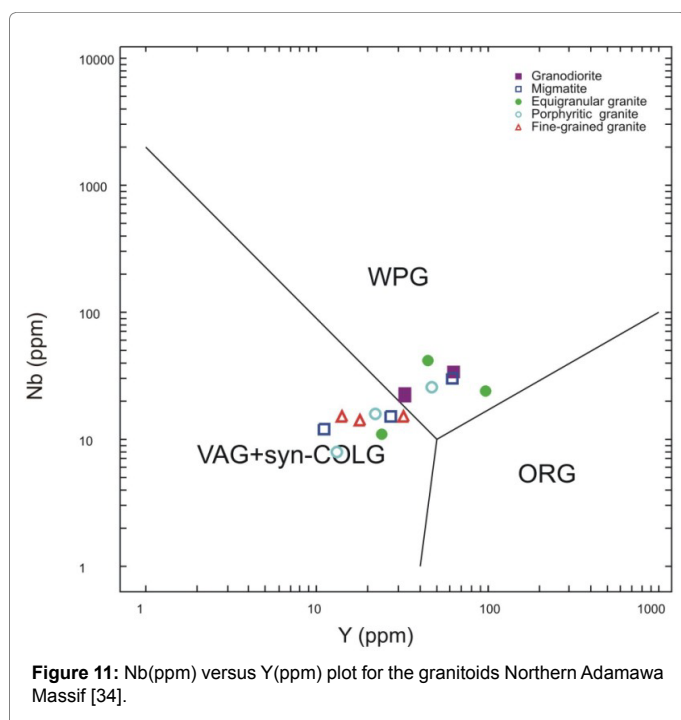


Figure 11: Nb(ppm) versus Y(ppm) plot for the granitoids Northern Adamawa Massif [34].

produce melts with Rb/Sr ratios <1.5 [41]. Granodiorite has higher Rb/Sr ratios than the granites. The higher Rb/Sr ratios in the granodiorite suggest that any fluid present during their formation must have low water content. It could also mean that the granites are residual from the granodiorite after fractionation of hornblende, biotite and minor plagioclase. However, considering the large volume of granites in the study area, we prefer the first possibility.

The REE patterns of the granitoids generally reflect the residual mineral assemblages of their source regions. The REE trends of the granodiorite and the granites are consistent with fractionation of biotite and plagioclase. The granitoids of the study area show REE trends that are characteristics of differentiated granites with moderate overall REE contents (TotREE = 492.66), a fractionated patterns [(La/Yb)_N = 15.55 on average], strongly fractionated LREE-enriched trends [(La/Sm)_N = 3.62 on average] with less fractionated HREE patterns [(Tb/Yb)_N = 1.52 on average] and significant negative Eu anomalies (Eu/Eu* = 0.41

on average). These REE trends agree with other field characteristics that the granitoids are differentiated and can be explained by fractional crystallization. Rocks with LREE-enriched trends but characterized by negligible EU anomalies would be consistent with the generation by partial melting from a mafic source in which amphibole and/or garnet are present as residual phases in the source [42]. Negligible/minor EU anomalies and fractionated REE trends are mostly compatible with the control of amphibole with minor plagioclase crystallization [43]. Therefore the appreciable EU anomalies observed for the granitoids of the study area suggest plagioclase fractionation.

Tectonic environment

Methodical trace element variation plots encompassing granites from practically all possible tectonic environments have been developed by Pearce et al, Harris et al and Whalen et al [34,35,44]. According to Pearce et al [34] and Pearce [36] granites can be discriminated on the basis of Nb, Y, Ta, Yb, and Rb trace element data into volcanic-arc, ocean ridge, within-plate and collisional types. On Nb versus Y diagram (Figure 11) [34] the granitoids plot in the within-plate (WPG), Volcanic-arc (VAG) and syn-collisional granite (syn-COLG) fields. Granitoids have average Y/Nb ratios greater than 1.2 which according to Eby [45] correspond to I-subtype granites generated in a subduction-related environment. Further, the enrichment of the granitoids in Nb, Y and Yb indicates affinity to the post-collisional granitoids.

Conclusion

Although there are slight mineralogical and geochemical differences between the granodiorite and the granites (e.g. Rb/Sr ratios lower in granodiorite than the granites) which may be attributed to their different petrologic histories, in general, the two rock units have similar geochemical characteristics. The rocks are characterized by a wide range in SiO₂, Calc-alkaline affinity, syn- to within-plate granite signatures, metaluminous to peraluminous composition and more K₂O-rich and hypersthene-poor comparable to fractionated I-type granitoids. The rocks display slightly fractionated to fractionated LREE, almost flat HREE patterns, with significant negative EU and Ba anomalies, Linear major element trends and progressive rise in SiO₂, K₂O, Rb and Rb/Sr ratios with depleting MgO, Fe₂O₃, CaO, TiO₂, Sr and Ba consistent with removal of plagioclase during fractionation of basic melts to yield silicic magma.

Based on field and petrochemical features, the granodiorites and the granites of northern Adamawa Massif are I-type, generated in a syn- to within-plate collision-related tectonic setting and genetically related to a common source by fractional crystallization dominated by the removal from the melt hornblende, plagioclase, biotite, K-feldspar and accessory phases such as apatite, epidote and zircon.

References

1. Geological Survey of Nigeria Agency (1996) Regional geological map of Nigeria, 1996 Edition.
2. Ferre E, Deleris J, Bouchez JL, Lar AU, Peucat JJ (1996) The Pan African reactivation of Eburnean and Archaean provinces in Nigeria: structural and isotopic data. J Geol Soc 153: 719-728.
3. Ekwueme BN (1985a) Petrology, geochemistry and Rb-Sr geochronology of metamorphosed rocks of Uwet area, southeastern Nigeria. Unpubl. PhD Thesis. University of Nigeria, Nsukka.
4. Ekwueme BN, Onyegocha AC (1986) Geochemistry of metasedimentary rocks of Uwet area, Oban massif, Southeastern Nigeria. Geol. Rundschau 75: 411-420.
5. Odigi MI, Okonny IP (1987) Application of radar imagery to structural and geological studies in Oban Massif, southeastern Nigeria. J Afr Earth Sci. 6: 275-280.

6. Ekwere SJ, Ekwueme BN (1991) Geochemistry of Precambrian Gneisses in the Eastern part of the Oban Massif, Southeastern Nigeria. *Geol Mijnb* 70: 105-114.
7. Ekwueme BN, Kroner A (1998) Single zircon evaporation ages from the Oban Massif, southeastern Nigeria. *J Afr Earth Sci*. 26: 195-205.
8. Ekwueme BN, Itaya T, Yabe H (2000) K-Ar ages of some metamorphic rocks of Oban Massif and their implications for the tectonothermal evolution of southeastern Nigeria. *Journ Min Pet Econ Geol* 95: 58-68.
9. Bassey NE (2007a) Brittle deformational features of Michika area, Hawal Basement complex, N.E. Nigeria. *Global Journal of Geological Sciences* 5: 51-54.
10. Obiefuna GI, Bassey NE, Ezeigbo HI, Duhu NS (1997) The geology and hydrogeology of Mubi and environs, N.E. Nigeria. *Water Resources* 8: 41-51.
11. Baba S (2009) Geology of Madagali area, Hawal Massif, N.E Nigeria. Unpubl. PhD Thesis, Federal University of Technology, Yola.
12. Ogunleye PO, Okujeni CD (1993) The geology and geochemistry of Zona uranium occurrence, Upper Benue Trough, N.E Nigeria. *Journal of Mining and Geology* 29: 175-181.
13. Burke KC, Dewey FJ (1972) Orogeny in Africa. In: T.F.J. Dessauvage and A.J. Whiteman (editors) *African Geology*. Geology Department, Univ. Ibadan, Nigeria.
14. Bertrand IML, Caby YR (1978) Geodynamic evolution of the Pan-African orogenic belt. A new interpretation of the Hoggar Shield (Algerian Sahara). *Geol. Rund* 67: 357-388.
15. Black R, Caby R, Pouchkine A, Bayer B, Bertrand JM, et al. (1979) Evidence for Late Precambrian plate tectonics in West Africa. *Nature* 278: 223-227.
16. Trumpette R (1979) The Pan-African Dahomeyide fold belt: a collision orogeny? (Abstract), 10th colloque de Geologic Africaine, Montpellier, pp.72-73.
17. Caby YR, Bertrand JM, Black R (1981) Pan African ocean closure and continental collision in the Hoggar-Iforas segment, Central Sahara. In: A Kroner (Editor) *Precambrian plate Tectonics*. Elsevier, Amsterdam, pp. 407-434.
18. Wright JB, Ogezi AEO (1977) Serpentinite in the Basement of Northwestern Nigeria. *Journ. Min. Geol.* 14: 34-37.
19. McCurry P, Wright JB (1977) Geochemistry of calc-alkaline volcanics in northwestern Nigeria, and a possible Pan-African suture zone. *Earth Planet. Sci. Lett.* 37: 90-96.
20. Holt RW, Egbuniwe IG, Fitches WR, Wright JB (1978) The relationships between low grade metasedimentary belts, calc-alkaline volcanism and the Pan-African orogeny in NW Nigeria. *Geol. Rand* 67: 631-646.
21. Ajibade AC, Woakes M, Rahaman MA (1989) Proterozoic crustal development in the Pan-African regime of Nigeria. In: C.A. Kogbe (Ed) *Geology of Nigeria 2nd Revised Edition*. Elizabethan publication company, Lagos, pp. 57-69.
22. Black R (1980) Precambrian of West Africa. *Episodes* 4: 3-8.
23. Turner DC (1983) Upper Proterozoic schist belts in the Nigerian sector of the Pan African province of West Africa. *Precamb. Res.* 21: 55-79.
24. Cox KJ, Bell JD, Pankhurst RJ (1969) *The interpretation of igneous rocks*. George Allen and Unwin Ltd, London, p450.
25. Streckeisen A (1976) To each plutonic rock its proper name. *Earth Sci. Rev.* 6: 181-217.
26. Frost BR, Barnes CG, Collins WJ (2001) A geochemical classification for granitic rocks. *Journal of Petrology* 42: 2003-2048.
27. Chappell BW, White AJR (1992) I- and S-type granites in the Lachlan Fold Belt. *Transaction Royal Society Edinburg Earth Science*, 83: 1-26.
28. Kleeman GL, Twist D (1989) The compositionally zoned sheet-like granite pluton of the Bushveld complex: evidence bearing on the nature on A-type magmatism. *Journal Petrology* 30: 1383-1414.
29. Chappell BW, White AJR (1974) Two contrasting granite types. *Pacific Geology* 8: 173-174.
30. Sun SS, Nesbitt RW (1978) Geochemical irregularities and genetic significance of ophiolitic basalts. *Geology* 6: 689-693.
31. Boynton WV (1984) Geochemistry of the rare earth elements: meteorite studies. In: Henderson P. (ed.), *Rare earth elements geochemistry*. Elsevier, pp 63-114.
32. Sun SS, McDonough WF (1989) Chemical and isotopic systematic of ocean basalts: implications for mantle composition and processes. In: Saunders A.D and Norry M.J (eds), *Magmatism in ocean basin*. Geol. Soc. London. Spec. Pub. 42: 313-345.
33. Weaver B, Tarney J (1984) Empirical approach to estimating the composition of the continental crust. *Nature* 310: 575-577.
34. Pearce JA, Harris NBW, Tindle AG (1984) Trace elements discrimination diagrams for the tectonic interpretation of granitic rocks. *Journal Petrology* 25: 956-983.
35. Harris NBW, Pearce JA, Tindle AG (1986) Geochemical characteristics of collision-zone magmatism. *Journal Geological Society, London, Special Publication* 19: 67-81.
36. Pearce JA (1996) Sources and settings of granitic rocks. *Episode* 9: 120-125.
37. Clarke DB (1996) Two centuries after Hutton's Theory of the Earth: the status of granite science. *Transaction Royal Society Edinburg Earth Sciences* 87: 353-359.
38. Chappell BW, White AJR (1977) Granitoids from the Moonbi district, New England batholiths, Eastern Australia. *Journ. Geol. Soc. Australia* 25: 267-283.
39. Tack L, Bowden P (1999) Post-collisional magmatism in the Central Damaran (Pan-African) Orogenic Belt, Western Namibia. *Journ. Afr. Earth Sc.* 28: 653-674.
40. Tindle AG, Pearce JA (1983) Assimilation and partial melting of continental crust: evidence from the mineralogy and geochemistry of autoliths and xenoliths. *Lithos.* 16: 185-202.
41. Harris NBW, Ayres M, Massey J (1995) The incongruent melting of muscovite: Implications for the geochemistry and extraction of granite magma. *Journal Geophysics Research* 100: 15777-15787.
42. Nagasawa H, Schnetzler CC (1971) Partitioning of rare earth, alkali and alkaline elements between phenocrysts and acidic igneous magma. *Geochimica Cosmochimica Acta.* 35: 953-968.
43. Hanson GN (1978) The applications of trace elements to the petrogenesis of igneous rocks of granitic composition. *Earth Planetary Science Letters* 38: 26-43.
44. Whalen JB, Currie KL, Chappell BW (1987) A-type granites: Geochemical characteristics, discrimination and petrogenesis. *Contributions Mineralogy Petrology* 95: 407-419.
45. Eby GN (1992) Chemical subdivision of the A-type granitoids: Petrogenetic and tectonic implications. *Geology* 20: 641-644.